HAPKE MODELING OF ASTEROID (25143) ITOKAWA USING HAYABUSA/AMICA DATA. Jian-Yang Li[1], L. Le Corre[1], V. Reddy[2], [1]Planetary Science Institute(jyli@psi.edu), [2]Lunar and Planetary Laboratory, University of Arizona.

Introduction: Asteroid (25143) Itokawa is a small near-Earth asteroid with a mean diameter of 320 m, with a spectral type of S that has surface composition similar to that of ordinary chondrite meteorites. Hayabusa mission rendezvoused with Itokawa starting from September 2005 and performed a detailed characterization of its basic properties, composition, mineralogy, geology, and returned samples from the surface of this asteroid to the ground for a detailed laboratory analysis. The spectral absorptions in 1- and 2-μm characteristic of mafic minerals (pyroxene, olivine) are clearly identified from the data and the general mineralogical properties of the asteroid has been studied [1]. Space weathering on the surface of Itokawa has been identified from the spectral color variations on this asteroid [2, 3]. The analysis of samples clearly shows the formation of nano-phased iron as the agent to cause the optical effects of space weathering, i.e., darkening and reddening, as well as the diminishing of spectral absorption features [4]. As part of an effort to study the mineralogical composition of the whole surface of this asteroid from multiband mosaic using the imaging data collected by the Asteroid Multiband Imaging Camera (AMICA) instrument, we performed a detailed photometric modeling with the Hapke model.

Data: AMICA is one of the three optical navigation multispectral cameras that were used to map the entire sunlit surface of the asteroid. The back-illuminated 1024×1000 pixel CCD operated has a field of view of 5.83º×5.69º. AMICA imaged the surface of Itokawa in seven color filters (0.38-1.0 μm) and one broadband clear filter centered at 0.65 μm. In this study, we used all images collected through seven color filters that had reconstructed pointing and trajectory information available. Images were imported in the Integrated Software for Imagers and Spectrometers (ISIS) developed by USGS and calibrated using the ISIS calibration routine *amicacal* (implemented as part of our previous work on AMICA data restoration [5]) that follows the processing steps described in [6]. Once the data were converted to *I*/*F*, and start time and pointing were updated, geometric backplanes were computed with standard ISIS routines using Itokawa's shape model in DSK format. These backplanes contain incidence angle, emission angle and phase angle values for every pixel in the image. To estimate the conversion factor for filter *zs*, we matched the *zs* images from the calibration image set used in [5] to a ground-based spectrum from NASA's Infrared Telescope Facility presented in [5]. The characteristics of the data are listed in Table 1.

Modeling: We used a five-parameter form of Hapke model to fit the data. With a maximum phase angle of the data <40º, a single-term Henyey-Greenstein (1pHG) phase function with an asymmetry factor, *g*, is sufficient to describe the phase function of the data. For opposition effects, we only include the shadow-hiding opposition effect with an amplitude parameter, B_0, and a width parameter, *h*. The other two parameters are the single-scattering albedo (SSA), *w*, and the roughness parameter, θ.

We started to fit the model to the *v*-band data due to the largest number of images and the much wider range of phase angle in this band compared to others. The photometric data are binned into scattering geometry bins (i, e, α) with bin size (1º, 1º, 0.2º) at α<1º, (2º, 2º, 1º) for 1º<α<4º, (4º, 4º, 2º) for 4º<α<20º, and (5º, 5º, 5º) for α>20º, where i, e, α are incidence angle, emission angle, and phase angle, respectively. The adaptive bin size in phase angle preserves the resolution in phase angle to facilitate the model fitting to the opposition surge, while significantly reduced the number of data points to be fitted. For all other bands, the bin size is (3º, 3º, 2º). All data points with i>80º or e>80º are excluded from fitting to avoid the relatively large uncertainties in the calculation of scattering geometry, and the abnormal behavior of photometric model near limb and terminator.

The fit to *v*-band data yields B_0=0.73, and *h*=0.024. The amplitude parameter is lower than the value derived from NIR, 0.87, and the width parameter is higher than previously derived, 0.010-0.014 [7]. It is not clear, though, whether [7] fixed their B_0 in model fitting, because they had the same modeled value for B_0 across the whole NIR wavelength in 0.85-2.4μm whereas their model uncertainties vary. The asymmetry factor *g*=-0.36, consistent with the NIR values [7]. The roughness parameter is 29º, comparable to 26º derived by [7]. The best-fit SSA is 0.39.

Next, we fixed B_0=0.73, and *h*=0.024 to fit the *b*-, *w*-, and *p*-bands, because the data in these bands do not cover opposition surge and therefore could not be used to derive the opposition parameters. The best-fit roughness parameters for these bands are all within a small range of 24º-29º. The *g* parameter has a very weak dependence on wavelength, range from -0.32 to -0.35.

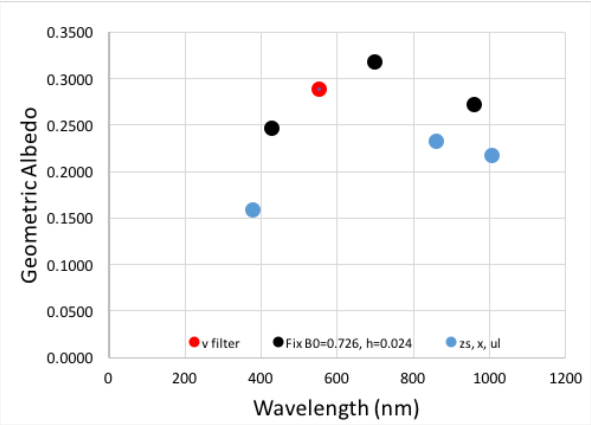

Figure 1. The geometric albedo spectrum of Itokawa based on our Hapke modeling.

Finally, we chose the *g* parameter for the *ul*-, *x*-, *zs*-bands based on the weak wavelength trend of *g* across the previously fitted four filters, *b*, *v*, *w*, and *p*, and fixed B_0, *h*, and *g*, and fixed θ=28º as an approximate average from other four bands, to fit those three bands to derive the SSA. All model results are listed in Table 1.

Discussion: The relative RMS (Table 1) are satisfying for *v*-band, but relatively high for *b*- and *w*-band, and almost unacceptable for *p*-band. The small RMS for *ul*-, *x*-, and *zs*-band could be due to the small number of data points available. Limiting input photometric data to *i*<75º and *e*<75º only slightly improve the RMS. Inspecting the dependence of the ratio between the modeled *I*/*F* and measured *I*/*F* on scattering geometry for *p*- and *zs*-band suggests some systematic bias with respect to *i* and *e*, suggesting possible changes in the disk-function relative to other bands, possibly caused by scattered light in the AMICA images [8]. Thus, the large model scattering in *p*-band could be related to scattered light.

The geometric albedo spectrum is shown in Fig. 1. The overall shape and the absolute scale of the geometric albedo spectrum of Itokawa from our modeling are reasonable for an S-type asteroid in the visible bands. In the NIR and IR bands, *x*, *p*, and *zs*, the variation in albedo must be due to modeling uncertainty, or due to scattered light, or absolute calibration (especially for filter *zs*). Setting the roughness parameter free in the model fitting for *zs* and *x* bands only slightly decreases the RMS, but does not improve the modeling results much. These are the bands that needs to be improved, probably with a better scattered light removal as outlined by Ishiguro (2014) [8], which we have not implemented in preparing our data for the photometric modeling presented here.

References: [1] Abe, M. et al. (2006) *Science, 312,* 1334. [2] Hiroi, T. et al. (2006) *Nature, 443,* 56. [3] Ishiguro, M. et al. (2007) *Meteorit. Planet. Sci., 42,* 1791. [4] Noguchi, T. et al. (2011) *Science, 333,* 1121. [5] Le Corre et al. (2017) 3rd planet. Data workshop, abstract #7033. [6] Ishiguro, M. (2010) *Icarus, 207,* 714-731. [7] Kitazato, K. et al. (2008) *Icarus, 194,* 137. [8] Ishiguro, M. (2014) *Publ. Astron. Soc. Japan, 66,* 55.

Acknowledgement: This work is supported by Planetary Missions Data Analysis Program award number NNX13AP27G.

Table 1. The characteristics of the photometric data that we used, and the best-fit Hapke model parameters. Values in parentheses are assumed and were kept fixed in the fitting. A_{geo} is geometric albedo, and A_{Bond} is Bond albedo.

Band	Center Wavelength (nm)	Min. Phase	Max. Phase	*w*	θ	*g*	B_0	*h*	A_{geo}	A_{Bond}	RMS%
ul	381	6.7º	9.2º	0.22	(28)	(-0.35)	(0.73)	(0.024)	0.16	0.062	6.1
b	429	5.8º	26.7º	0.34	27.6	-0.35	(0.73)	(0.024)	0.25	0.10	9.2
v	553	0.0º	38.6º	0.39	28.9	-0.35	0.73	0.024	0.29	0.12	4.5
w	700	5.8º	27.0º	0.47	24.1	-0.32	(0.73)	(0.024)	0.32	0.15	9.5
x	861	6.7º	9.2º	0.35	(28)	(-0.33)	(0.73)	(0.024)	0.23	0.10	4.8
p	960	6.7º	27.0º	0.40	25.2	-0.33	(0.73)	(0.024)	0.27	0.13	13.8
zs	1008	6.7º	9.2º	0.32	(28)	(-0.33)	(0.73)	(0.024)	0.22	0.094	5.1